

Deconvolution of isotope signals from bundles of multiple hairs

Christopher H. Remien · Frederick R. Adler ·
Lesley A. Chesson · Luciano O. Valenzuela ·
James R. Ehleringer · Thure E. Cerling

Received: 3 April 2013 / Accepted: 9 April 2014
© Springer-Verlag Berlin Heidelberg 2014

Abstract Segmental analysis of hair has been used in diverse fields ranging from forensics to ecology to measure the concentration of substances such as drugs and isotopes. Multiple hairs are typically combined into a bundle for segmental analysis to obtain a high-resolution series of measurements. Individual hair strands cycle through multiple phases of growth and grow at different rates when in the growth phase. Variation in growth of hair strands in a bundle can cause misalignment of substance concentration between hairs, attenuating the primary body signal. We developed a mathematical model based on the known physiology of hair growth to describe the signal averaging caused by bundling

Communicated by Hannu J. Ylonen.

Electronic supplementary material The online version of this article (doi:[10.1007/s00442-014-2945-3](https://doi.org/10.1007/s00442-014-2945-3)) contains supplementary material, which is available to authorized users.

C. H. Remien (✉)
National Institute for Mathematical and Biological Synthesis,
University of Tennessee, Knoxville, TN 37996, USA
e-mail: cremien@nimbios.org

F. R. Adler
Department of Mathematics, University of Utah, Salt Lake City,
UT 84112, USA

F. R. Adler · L. A. Chesson · L. O. Valenzuela · J. R. Ehleringer ·
T. E. Cerling
Department of Biology, University of Utah, Salt Lake City,
UT 84112, USA
e-mail: thure.cerling@utah.edu

L. A. Chesson · L. O. Valenzuela · J. R. Ehleringer · T. E. Cerling
IsoForensics, Salt Lake City, UT 84108, USA

T. E. Cerling
Department of Geology, University of Utah, Salt Lake City,
UT 84112, USA

multiple hairs for segmental analysis. The model was used to form an inverse method to estimate the primary body signal from measurements of a hair bundle. The inverse method was applied to a previously described stable oxygen isotope chronology from the hair of a murder victim and provides a refined interpretation of the data. Aspects of the reconstruction were confirmed when the victim was later identified.

Keywords Stable isotope · Mathematical model · Inverse methods

Introduction

Organic and inorganic substances in mammals are incorporated into hair, remaining inert for relatively long periods of time (Henderson 1993). Human forensic applications have long been recognized, as drugs, metabolites, toxins, and poisons are incorporated into hair at the time of formation (Cooper et al. 2011; Sachs 1997; Selavka and Rieders 1995; Staub 1995). More recently, ecologists and anthropologists have used stable isotopes in hair to infer information about an animal's history, including diet, migration, and nutritional status (Martínez del Rio 2009; Crawford et al. 2008; Wolf 2009; Cerling et al. 2009; Petzke et al. 2010; Schwertl et al. 2003). While the growth of hair is approximately linear, allowing the measurement of long-term chronology through segmental sampling, individual hairs typically have too low linear density to allow high-resolution sampling of a single hair. Sample sizes vary, but segments for drug testing are typically between 10 and 30 mm (Cooper et al. 2011) and generally require 1–300 mg of hair (Wainhaus et al. 1998). Stable isotope ratios of hydrogen, carbon, nitrogen, oxygen, and sulfur require ca. 200, 50, 300, 200, and 900 µg, respectively. To achieve these masses for animals with hair of

relatively low linear density, such as humans, multiple hair strands are typically aligned at the root and combined into a single bundle for analysis (Cooper et al. 2011; Lebeau et al. 2011). The challenge is to mathematically extract the true chemical signal recorded in hair given variations in growth rate and stasis, because these processes will tend to blur, or average, the temporal information recorded in hair.

Two distinct processes can cause misalignment between individual hair strands in a bundle: variation in growth phase (Sachs 1995) and variation in growth rate (Lebeau et al. 2011). Each hair follicle cycles through three distinct phases of growth (Chase 1954; Kligman 1959). In humans, approximately 90 % of hairs are typically in the anagen, or growth, phase, which lasts for 48–72 months. The anagen phase is followed by a brief catagen phase, during which the follicle stops producing hair. The hair then enters the telogen, or resting, phase during which the follicle and hair remain dormant for 2–6 months, until the hair is shed. Variation of growth rate between individual hairs in the growth phase can also blur the measured signal of a hair bundle (Lebeau et al. 2011). The intraindividual coefficient of variation of hair growth in humans is about 0.1 (Myers and Hamilton 1951; Lee et al. 2005), and similar variation has been observed in horses (West et al. 2004) and elephants (Wittemyer et al. 2009). Because individual hair strands vary in growth, signal details present in a single hair may not be captured in hair bundle measurements due to averaging misaligned hair strands in a bundle.

Previous studies implicitly assume that the measured bundle signal is equivalent to the signal of a single hair in the growth phase with average growth rate. Given known physiology of hair growth, we assume that the phase of growth and growth rates of individual hairs will vary within a bundle. We have developed a mathematical model of hair growth that describes the relationship between the signal of a bundle of hairs and the primary body signal (e.g., the isotopic pool in the body at equilibrium with hair). The model is based on an estimation of uncertainty in time since formation, or age, of the hair at a given length from the root. We used the model to develop an inverse method to estimate the primary body signal from hair bundle measurements. Our inverse method was applied to a previously described stable oxygen isotope chronology from a hair bundle of a murder victim (Ehleringer et al. 2010) and provides a refined interpretation of the original data.

Methods

Model formulation

Mapping single hair signal to hair bundle measurements

Let $\phi(t)$ be the time-dependent primary body signal (e.g., drug, metabolite, isotope, etc.) to the hair. The function

$\phi(t)$ refers to the input signal to the hair (e.g., the isotopic pool in the body at equilibrium with hair), not the input signal to the body (e.g., drinking water, drug dosage history, etc.), and is assumed to be equivalent to the signal of a single hair in the growth phase with the average growth rate. The expected bundle signal as a function of length is

$$\psi(l) = \int \lambda(l, \tau) \phi(\tau) d\tau, \quad (1)$$

where $\lambda(l, a)$ is the probability density function of time since formation, or age, of a hair at length l from the root given that the total length of the hair is at least l and the hair has not yet been shed. The kernel λ quantifies the length-dependent uncertainty in age.

Evaluation of $\lambda(l, a)$

Let $\lambda(l, a)$ be the probability density function for the random variable time since formation, or age, A , of hair at length l from the root, given that the hair has not been shed, and the total length of the hair is at least l . We assume that hair grows at constant random rate R for random time S , and then rests for random time T before being shed. We found the distribution of λ in terms of the probability distributions of R , S , and T denoted in Table 1 to be:

$$\begin{aligned} \lambda(l, a) = & g(l) \frac{l}{a^2} h\left(\frac{l}{a}\right) \\ & + (1 - g(l)) \int_0^a \frac{l}{(a - \tau)^2} \kappa(\tau) h\left(\frac{l}{a - \tau}\right) d\tau, \end{aligned}$$

where

$$g(l) = \int_0^\infty h(r) \int_{l/r}^\infty \int_{l/r}^v \frac{s - l/r}{v - l/r} f_S(s) f_T(v - s) ds dv dr$$

Table 1 Definitions of distributions used in modeling

Distribution	Description
h	Probability distribution function for the growth rate of hair, R
H	Cumulative distribution function for the growth rate of hair, R
f_S	Probability distribution function for the time spent in growth phase, S
F_S	Cumulative distribution function for the time spent in growth phase, S
f_T	Probability distribution function for the time spent in resting phase, T
F_T	Cumulative distribution function for the time spent in resting phase, T

Table 2 Parameters and distributions used in modeling

Parameter	Description	Value
γ	Fraction of hairs in resting phase	0.05, 0.1, 0.3
α	Coefficient of variation of hair growth rate	0.05, 0.1, 0.25
β	Mean hair growth rate	1 cm/month (Lebeau et al. 2011; Myers and Hamilton 1951)
v	Mean time from beginning of growth phase to hair shedding	66 months (Sachs 1995)
Distribution	Description	Value
h	Hair growth rate probability density function	$N(\beta, (\beta\alpha)^2)$
f_s	Time in growth phase probability density function	$N(v(1 - \gamma), (0.1v(1 - \gamma))^2)$
f_T	Time in resting phase probability density function	$N(v\gamma, (0.1v\gamma)^2)$

and

$$\kappa(a) = \int_a^{\infty} \frac{f_T(x)}{x} dx.$$

Refer to the Electronic Supplemental Material for a complete derivation.

Averaging due to sample interval

Signal attenuation also occurs by combining material over the sample length to obtain the mass of material required for analysis. In the case of sampling a single hair that is in the growth phase with fixed growth rate r , the expected measured signal, $f(l)$, is the average of the time-dependent primary body signal, $\phi(t)$, converted to length, over the sample length v :

$$f(l) = \frac{r}{v} \int_{l/r-v/(2r)}^{l/r+v/(2r)} \phi(\tau) d\tau.$$

The center of the samples are at lengths $l = (2i - 1)v/2$, where i is a positive integer. Sampling a bundle containing a large number of hairs allows for small sample length, so the measured signal of a bundle of hairs approaches $\psi(l)$.

Inverse method

To estimate the time-dependent input signal $\phi(t)$ from measurements of $\psi(l)$, we discretized Eq. 1 into the matrix vector equation $Kf = d$, where f is a discretization of $\phi(t)$, d is a vector containing the measured values of $\psi(l)$, and K is an $m \times n$ matrix. The discretization of $\phi(t)$ was chosen to have the same step size as the measurements d .

As in the estimation of a primary input signal from a measured stable isotope tooth enamel signal described by Passey et al. (2005), we used Tikhonov regularization to invert K , yielding the estimation

$f_{\text{est}} = f_{\text{guess}} + K^T [KK^T + \varepsilon^2 I]^{-1} [d - Kf_{\text{guess}}]$, where I is an identity matrix, f_{guess} is an a priori reference vector, and ε is a scalar regularization parameter. The reference vector f_{guess} was chosen to be a vector containing the mean value of the measurements d .

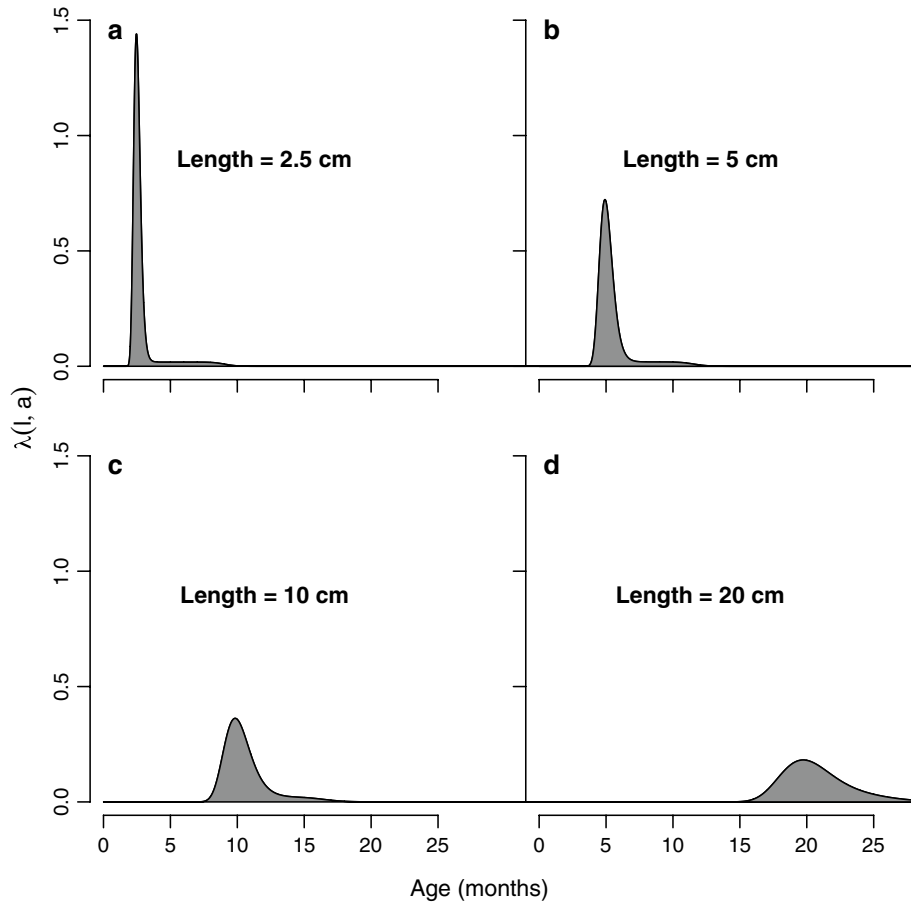
The damping factor ε was chosen using generalized cross-validation. The chosen ε minimizes the GCV functional $\text{GCV}(\varepsilon) = \frac{\frac{1}{n} \|r_\varepsilon\|^2}{\left[\frac{1}{n} \text{trace}(I - A_\varepsilon) \right]^2}$, where $r_\varepsilon = Kf_{\text{est}} - d$ and $A_\varepsilon = K(K^T K + \varepsilon^2 I)^{-1} K^T$ (Vogel 2002).

Results

Using the distributions in Table 2, the model depends on two parameters: γ is the fraction of hairs in the resting phase (catagen and telogen), and α is the coefficient of variation of hair growth rate. The integral transform kernel, $\lambda(l, a)$, is the probability density as a function of time since formation, or age, of hair at a given length from the root and describes the amount of signal attenuation in the hair bundle signal. Using the distributions in Table 2, the kernel $\lambda(l, a)$, with $\gamma = 0.1$ and $\alpha = 0.1$, is shown in Fig. 1. We varied γ and α to assess how these parameters affect $\lambda(l, a)$ (Fig. 2). A high fraction of hairs in the resting phase, γ , results in high variance in age of hair at all lengths and a mean age that is higher than the length divided by the mean growth rate. A high coefficient of variation of hair growth rate, α , results in increasing variance of age with length. The distribution of age dictates the uncertainty in time when sampling a single hair and also the expected amount of averaging from sampling a bundle of multiple hairs.

The assumed stable isotope primary input signals in Figs. 3 and 4 are from single elephant tail hairs sampled at 5 mm intervals. Elephants have thick hairs with high linear density, allowing for high-resolution sampling of a single hair. The data in Fig. 3 represent an individual migrating between two areas with different $\delta^{15}\text{N}$ values for vegetation

Fig. 1 The kernel $\lambda(l, a)$ at lengths 2.5, 5, 10, and 20 (a–d), respectively, describes the variation of time since formation, or age, at a given length from the root



and, thus, an abrupt change in hair $\delta^{15}\text{N}$ occurs at each migration event (Cerling et al. 2006); transitions between areas were made in less than 12 h based on GPS-tracking data. Migration events result in a signal approximating a step function. Data from this individual are previously unpublished, but the individual had behavior analogous to that described by Cerling et al. (2006). We extended this signal periodically to create a longer signal. The data in Fig. 4 are from Cerling et al. (2009) and represents gradual diet transitions coinciding with two rainy seasons per year.

We compared the expected value of the signal from sampling a bundle of hairs that contains hairs with varying growth rates and phases, with $\gamma = 0.1$ and $\alpha = 0.1$, to sampling a single hair that has a growth rate of 1 cm/month and sample length $v = 1.5$ cm (Fig. 3). The primary body signal refers to the signal of the body pool at equilibrium with hair and is the signal of a single hair in the growth phase with average growth rate. Signal attenuation occurs when sampling a single hair because of combining material over the sample length. Combining multiple hairs into a bundle for sampling attenuates the primary body signal because of varying growth phases and growth rates of hairs in the bundle. Signal details of sufficiently short duration are highly damped and are not captured in the bundle signal because

of averaging. When sampling a single hair, events of duration shorter than the sample length may not be recorded. Additionally, when sampling a single hair, there is considerable uncertainty in assigning time to length since the exact growth rate and phase of growth of the sampled hair is not usually known.

To test the ability of the inverse method to accurately reconstruct a primary body signal from measurements, we used the forward hair bundle model, with $\gamma = 0.1$ and $\alpha = 0.1$, to create a synthetic measured bundle signal from an assumed primary body signal. We then used the inverse method to estimate the primary body signal from the synthetic bundle signal (Fig. 4). The estimated primary body signal is more similar to the primary body signal (correlation coefficient $r^2 = 0.81$) than the measured hair bundle signal is to the primary body signal (correlation coefficient $r^2 = 0.43$). High frequency details are lost in the estimated input signal, but the general pattern remains well estimated.

Application of inverse method to murder victim data

We used Tikhonov regularization to reconstruct the $\delta^{18}\text{O}$ primary body signal of an unidentified murder victim from

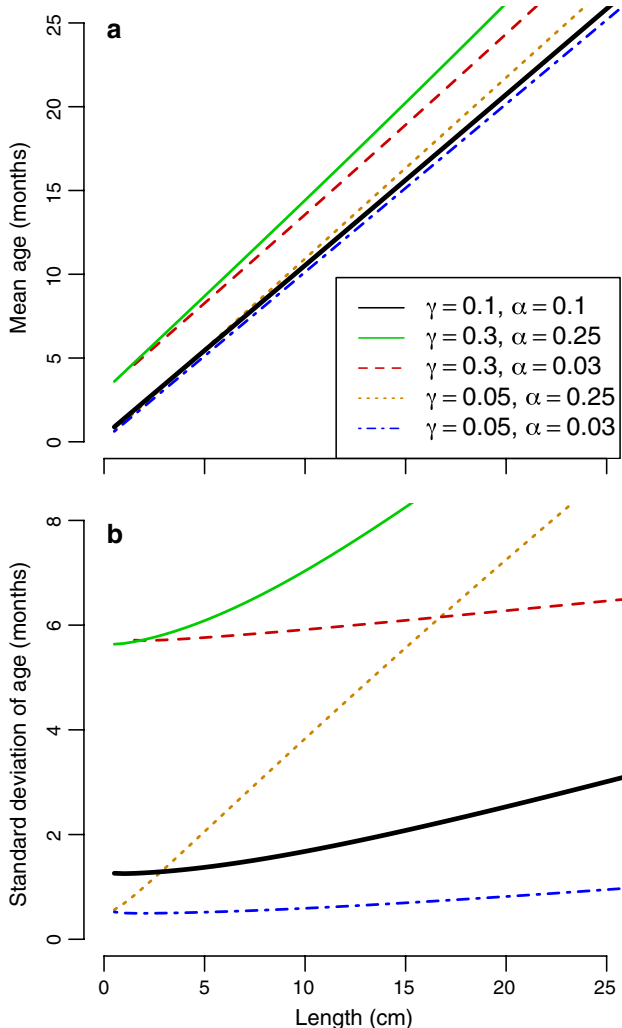


Fig. 2 Mean (a), and standard deviation (b), of time since formation, or age, of hair at a given length from the root for various values of fraction of hairs in the resting phase, γ , and coefficient of variation of hair growth rate, α

stable isotope measurements of the organic component of a hair bundle, with $\gamma = 0.1$ and $\alpha = 0.1$, (Fig. 5a, b) (Ehleringer et al. 2010; Kennedy et al. 2011). The murder victim, nicknamed by law enforcement “Saltair Sally,” was found near Salt Lake City, Utah in October 2000. Oxygen stable isotope measurements of the organic component of hair can be used to determine the time-dependent geographic region-of-origin because oxygen isotopes in drinking water vary with location (Bowen and Wilkinson 2002) and are incorporated into hair (O’Brien and Wooller 2007; Ehleringer et al. 2008).

The confidence interval for the estimated primary body signal was obtained by inverting data with noise added to each measurement, representing uncertainty related to analysis. We created 1,000 replicates of measurements by adding normally distributed noise with mean zero and standard

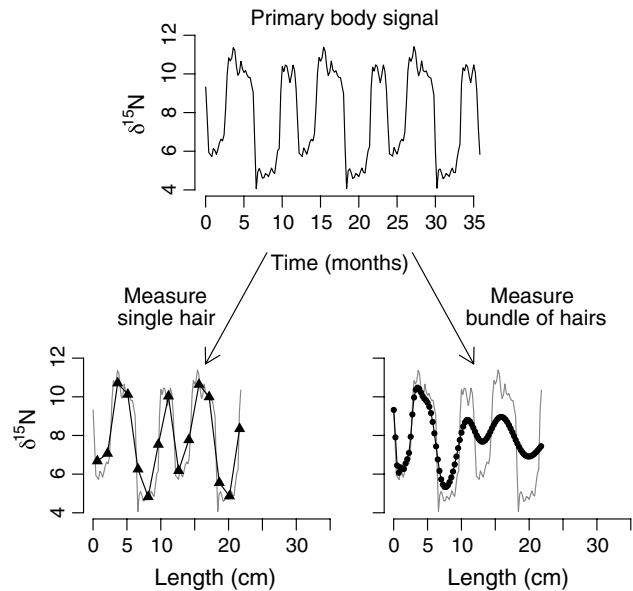


Fig. 3 Expected length-dependent single hair signal and hair bundle signal derived from our mathematical model using an assumed time-dependent primary body signal. Time indicates months prior to formation of hair at root, length indicates cm from root. The signal of the measured bundle of hairs is highly attenuated relative to the primary body signal

deviation of 0.15 ‰ to each measurement. For each set of measurements with added noise, we selected a regularization parameter using generalized cross-validation, and performed the inversion using Tikhonov regularization to estimate the primary body signal. We excluded two estimates of the primary body signal because their isotope values lay outside the biologically feasible range of 5–18 ‰. The shaded region corresponds to $\delta^{18}\text{O}$ within two standard deviations of the mean estimated primary body signal. We tested the sensitivity of the inversions to changes in γ and α by increasing and decreasing γ and α by 50 % and performing the inversions as above. The amplitude of peaks are most sensitive to α , the coefficient of variation of hair growth (Figs. S3, S4, S5, and S6). A high value of α leads to larger amplitude transitions, while a low value of α leads to inversions that are more damped. The general pattern, however, is robust to changes in γ and α .

The model inversion yields an estimate of the primary body pool at equilibrium with the hair, not the input signal to the body. The body equilibrium signal refers to the primary body signal if it were in instantaneous equilibrium with the input. The body equilibrium signal can be reconstructed using a previously described method based on multiple pools with first order kinetics contributing to the primary body pool that is at equilibrium with hair (Cerling et al. 2004, 2007). For application to the murder victim data, we used a single pool with half-life of 7 days,

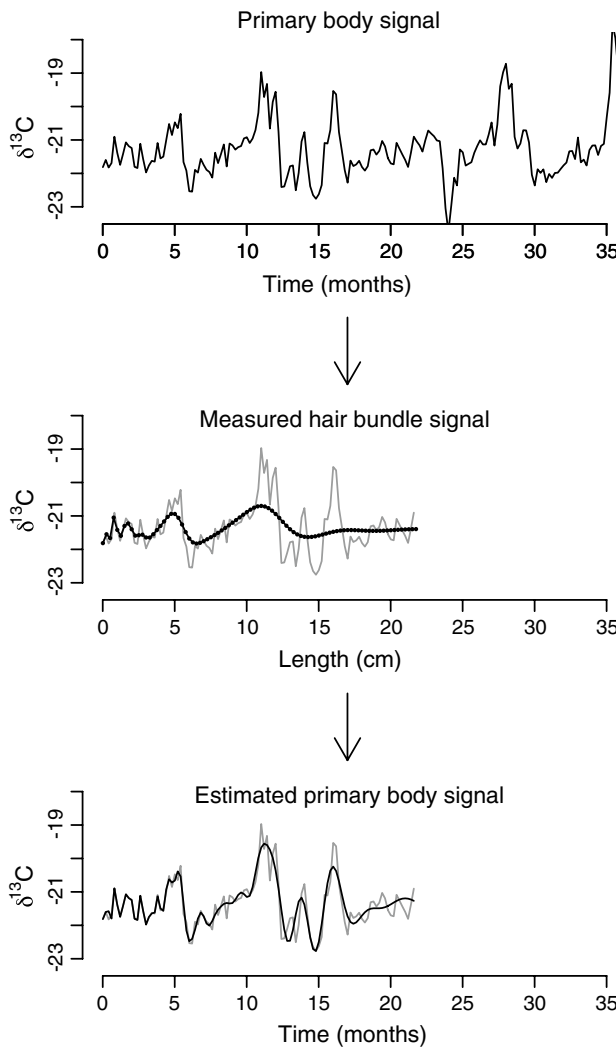


Fig. 4 A primary body signal that is attenuated from sampling a bundle of hairs can be partially reconstructed from measurements using inverse methods. Time indicates months prior to formation of hair at root, length indicates cm from root

which is consistent with observations of hair oxygen stable isotopes in humans (calculated from O'Brien and Wooller 2007; Ehleringer et al. 2008). In this case, the estimated equilibrium signal is very similar to the estimated primary body signal because of rapid turnover of the primary body pool relative to changes in the input signal (refer to the Electronic Supplemental Material for more detail).

Region-of-origin maps were created in two steps. For each region, we used the semi-mechanistic model by Ehleringer et al. (2008) to predict drinking water $\delta^{18}\text{O}$ values required to produce the hair isotope ratio, with an added 0.5 ‰ to either side of the value. Once the maximum and minimum $\delta^{18}\text{O}$ values of drinking water were predicted for each isotopic region, we used the $\delta^{18}\text{O}$ tap water isoscape produced by Bowen et al. (2007) for the contiguous United

States to identify regions with isotope values matching our predicted range. Regions with matching isotope values were highlighted in color using ArcGIS 9.3.1®.

The data were originally interpreted as movement between three isotopically distinct geographic regions, Regions 1, 2, and 3, corresponding to measured $\delta^{18}\text{O}$ values of approximately 9.9, 8.4, and 9.2 ‰, respectively (Ehleringer et al. 2010). The transitions from Region 1 to Region 2 and from Region 2 to Region 1 at about 20 and 15 cm, respectively, occur over multiple cm (or equivalently multiple months) of growth, slow movement between geographic regions. The transitions from Region 1 to Region 3 and from Region 3 to Region 1 at about 9 and 5 cm, respectively, occur over a short length 10 interval, rapid movement between geographic regions. Region 1 is consistent with the location where the victim was found, Salt Lake City, UT.

The estimated equilibrium signal differs from the measured hair bundle in several important ways (Figs. 5a, b, S1, and S2). Transitions between isotopically distinct regions are more rapid, with more time spent in each region. Region 2* and Region 3* have lower $\delta^{18}\text{O}$ than Region 2 and Region 3, respectively, and may correspond to different geographic regions (Fig. S1). Regions 2* and 3* have considerable overlap (Fig. S2), suggesting that they may correspond to the same geographic location. Region 1 is isotopically similar in both the measurements and the estimated equilibrium signal, and the $\delta^{18}\text{O}$ is consistent with the location where the victim was found. The estimated equilibrium signal has a new short duration region, Region 4, with $\delta^{18}\text{O}$ of about 11 ‰ that does not appear in the measured hair bundle signal. Plotted maps were restricted to the western United States. Region 4 also contains a small region in the northeast United States as well as parts of Canada.

Discussion

Multiple hairs that may be in different growth phases and have different growth rates are typically combined into a single bundle of hairs for segmental analysis. We have developed a mathematical model that describes the signal averaging caused by bundling hairs for analysis as well as an inverse method to estimate the primary body signal from measurements of a hair bundle. If the growth rates of hairs within a bundle vary substantially or a high proportion of hairs are in the resting phase of hair growth, the measured hair bundle signal is highly averaged relative to the primary body signal, which may lead to misinterpretation of the signal.

Our model is based on uncertainty in time since formation, or age, of hair a given length from the root. Assigning times to length when sampling a single hair strand also

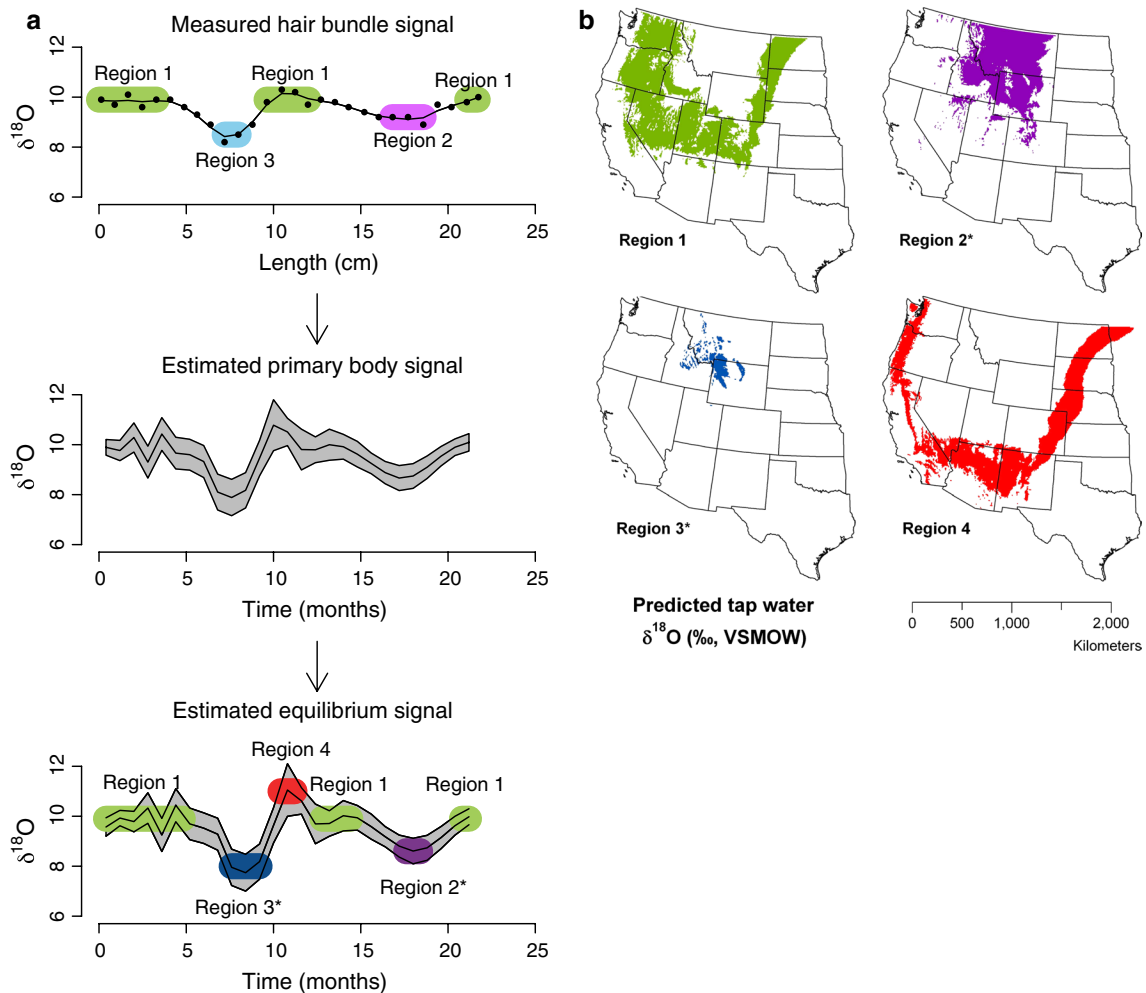


Fig. 5 **a** Estimated primary body signal and equilibrium signal from hair $\delta^{18}\text{O}$ measurements of a previously described hair bundle of a murder victim (Ehleringer et al. 2010; Kennedy et al. 2011). **b** Tap water maps for geographic regions predicted by the estimated equilibrium signal

relies on an estimation of length-dependent age variation. High variation in growth rates or a high proportion of hairs in the resting phase of hair growth leads to high uncertainty in assigning time to measurements along the length of a single hair strand.

The determination of whether to bundle hairs or sample a single hair depends on the research question. If precise timing of an event is critical or high-resolution sampling is desired to capture events in the recent past, multiple hairs should be combined into a bundle to decrease sample length and reduce uncertainty in the time corresponding to measurements. If multiple hairs are to be combined, it is preferred to combine many hairs rather than few, as the uncertainty in the bundle signal decreases with the number of hairs. If the amplitude of a long duration event is more important or an individual hair strand has high enough linear density to allow for a high-resolution sample interval, sampling a single hair strand may result in less signal

averaging than sampling a bundle of hairs. When sampling a single hair, however, there may be high uncertainty in assigning time to measurements.

The inverse method we developed allows for the estimation of the primary body signal from a measured hair bundle signal. The method is especially useful in situations where the primary body signal is averaged, but characteristics of the signal remain. If the averaging is significant enough, however, noise may dominate, preventing meaningful reconstruction of the primary body signal.

It may be possible to minimize signal averaging from bundling multiple hairs by ensuring hairs are in the growth phase. Van Scott et al. have described a technique to examine a hair's follicle to determine its phase of growth (Van Scott et al. 1957), though this is only possible if a hair's root can be observed (i.e., hair was plucked rather than cut). Excluding hairs in the resting phase from a bundle has been shown to reduce the growth cycle error in hair stable

isotope analysis (Williams et al. 2011). This can be incorporated into our model by reducing γ , the fraction of hairs in the resting phase, which results in less signal averaging. If the hair has never been cut, selecting hairs for analysis with small total length also increases the likelihood of hair being in the growth phase. Since each hair grows for a period of time before shedding, hairs with small total length are more likely to be in the growth phase. However, the bundled signal will still be attenuated due to variation in growth rate of individual hairs.

We applied our inverse method to a previously described (Ehleringer et al. 2010; Kennedy et al. 2011) oxygen stable isotope chronology from the organic component of the hair of a murder victim. The signal obtained from the inverse method is an estimate of the $\delta^{18}\text{O}$ of the primary body pool that is in equilibrium with the hair, rather than the time-dependent isotopic composition of drinking water. Applying a model of turnover of the primary body pool $\delta^{18}\text{O}$ to the estimated primary body signal provides an estimate of the equilibrium signal. This further sharpens the transitions between regions, though the effect is small due to the relatively rapid turnover of oxygen isotopes in the primary body pool at equilibrium with hair. In cases where turnover of the body pools at equilibrium with hair is slow (e.g., carbon (Ayliffe et al. 2004) and nitrogen isotopes (Sponheimer et al. 2003)), the signal attenuation caused by turnover of the body pools may be larger than that caused by bundling multiple hairs. The search maps determined by the estimated equilibrium signal differ from previously published interpretations in several important ways. Transitions between isotopically distinct regions are more rapid, and predicted regions have slightly different $\delta^{18}\text{O}$. An additional region of short duration with relatively high $\delta^{18}\text{O}$ is present in the estimated equilibrium, that may have been averaged by measuring a bundle of multiple hairs.

The murder victim has since been identified through DNA analysis as Nikole Bakoles. There are several insights and consistencies between model predictions and observations from Nikole's life. Nikole was a known traveler, and the hair record shows this. Nikole is known to have spent time with her parents, and this shows up in the Seattle-Tacoma predictions. She was a resident of Salt Lake County, who moved in and out of the area, and this shows up in the isotope record of her hair. A major unknown is that the model predicts a third area, north of Salt Lake City. At the moment, investigators do not know about these travels.

In some animals, hair grows seasonally. If the growth phases of individual hair strands are correlated, the signal of a hair bundle will have lower attenuation relative to the primary body signal because hairs are likely to be in the same growth phase. There will, however, still be variation in hair growth rate between hairs, and variation in

hair growth rate between hairs may have a larger effect on attenuating the signal (Supplemental Figures S1, S2, S3, and S4).

Similar methods may also be used to estimate uncertainty in time since formation, when time cannot be constrained using other methods, in other length-dependent measurements of ecological tape recorders, such as measurements of nails, horn, or tropical trees lacking growth rings. Additionally, similar probability density functions may be useful for estimating the uncertainty in age of an animal or plant from size or length. The details of these methods will depend on growth characteristics. Other biological systems, such as cell-cycle dependent processes, also rely on inverse methods to estimate individual signal from population-level measurements (Lu et al. 2003; Bar-Joseph et al. 2004; Rowicka et al. 2007; Siegal-Gaskins et al. 2009). In these models, variation in cell-cycle phase of individual cells can result in important differences between population measurements and individual cell dynamics.

Hair records the concentration of drugs, toxins, metabolites, and stable isotopes in the body as it grows. Segmental analysis of a bundle of hair allows for the construction of a high-resolution record of the history of an animal. However, variation in the growth of individual hair strands can distort the relation between measurements and the actual history of the animal. Our mathematical model provides an estimate of uncertainty in time since formation, or age, of a hair strand a given length from the root as well as an inverse method to estimate the time-dependent primary body signal (e.g., drug, metabolite, isotope, etc.) from segmental analysis of a bundle of hairs, based on measurable growth characteristics of individual hair strands.

Acknowledgments CHR conducted this work as a University of Utah Research Training Group Fellow through NSF award #EMSW21-RTG and as a Postdoctoral Fellow at the National Institute for Mathematical and Biological Synthesis, an Institute sponsored by the National Science Foundation, the US Department of Homeland Security, and the US Department of Agriculture through NSF Award #EF-0832858, with additional support from The University of Tennessee, Knoxville.

References

- Ayliffe LK, Cerling TE, Robinson T, West AG, Sponheimer M, Passey BH, Hammer J, Roeder B, Dearing MD, Ehleringer JR (2004) Turnover of carbon isotopes in tail hair and breath CO_2 of horses fed an isotopically varied diet. *Oecologia* 139:11–22
- Bar-Joseph Z, Farkash S, Gifford DK, Simon I, Rosenfeld R (2004) Deconvolving cell cycle expression data with complementary information. *Bioinformatics* 20:23–30
- Bowen GJ, Wilkinson B (2002) Spatial distribution of ($\delta^{18}\text{O}$) in meteoric precipitation. *Geology* 30(4):315–318
- Bowen GJ, Ehleringer JR, Chesson LA, Stange E, Cerling TE (2007) Stable isotope ratios of tap water in the contiguous United States. *Water Resour Res* 43:1–12

- Cerling TE, Passey BH, Ayliffe LK, Cook CS, Ehleringer JR, Harris JM, Dhadha MB, Kasiki SM (2004) Orphans' tales: seasonal dietary changes in elephants from Tsavo National Park, Kenya. *Palaeogeogr Palaeoclim Palaeoecol* 206:367–376
- Cerling TE, Wittemyer G, Rasmussen HB, Vollrath F, Cerling CE, Robinson TJ, Douglas-Hamilton I (2006) Stable isotopes in elephant hair document migration patterns and diet changes. *Proc Natl Acad Sci (USA)* 103(2):371–373
- Cerling TE, Ayliffe LK, Dearing MD, Ehleringer JR, Passey BH, Podlesak DW, Torregrossa AM, West AG (2007) Determining biological tissue turnover using stable isotopes: the reaction progress variable. *Oecologia* 151:175–189
- Cerling TE, Wittemyer G, Ehleringer JR, Remien CH, Douglas-Hamilton I (2009) History of animals using isotope records (HAIR): a 6-year dietary history of one family of African elephants. *Proc Natl Acad Sci (USA)* 106:8093–8100
- Chase HB (1954) Growth of the hair. *Physiol Rev* 34:113–126
- Cooper GAA, Kronstrand R, Kintz P (2011) Society of hair testing guidelines for drug testing in hair. *Forensic Sci Int* 218(1–3):20–24
- Crawford K, McDonald RA, Bearhop S (2008) Applications of stable isotope techniques to the ecology of mammals. *Mamm Rev* 38(1):87–107
- Ehleringer JR, Bowen GJ, Chesson LA, West AG, Podlesak DW, Cerling TE (2008) Hydrogen and oxygen isotope ratios in human hair are related to geography. *Proc Natl Acad Sci (USA)* 105(8):2788–2793
- Ehleringer JR, Thompson AH, Podlesak DW, Bowen GJ, Chesson LA, Cerling TE, Park T, Dostie P, Schwarcz H (2010) A framework for the incorporation of isotopes and isoscapes in geospatial forensic investigations. In: West JB et al. (eds) Isoscapes: understanding movement, pattern, and process on earth through isotope mapping, chapter 17. Springer, p 357–387. doi:10.1007/978-90-481-3354-3_17
- Henderson GL (1993) Mechanisms of drug incorporation into hair. *Forensic Sci Int* 63:19–29
- Kennedy CD, Bowen GJ, Ehleringer JR (2011) Temporal variation of oxygen isotope ratios ($\delta^{18}\text{O}$) in drinking water: implications for specifying location of origin with human scalp hair. *Forensic Sci Int* 208:156–166
- Kligman AM (1959) The human hair cycle. *J Invest Dermatol* 33:307–316
- Lebeau MA, Montgomery MA, Brewer JD (2011) The role of variations in growth rate and sample collection on interpreting results of segmental analyses of hair. *Forensic Sci Int* 210:110–116
- Lee SH, Kwon OS, Oh JK, Park WS, Moon SE, Eun HC (2005) Bleaching phototrichogram: an improved method for hair growth assessment. *J Dermatol* 32(10):782–787
- Lu P, Nakorchevskiy A, Marcotte E (2003) Expression deconvolution: a reinterpretation of DNA microarray data reveals dynamic changes in cell populations. *Proc Natl Acad Sci (USA)* 100:10370–10375
- Martínez del Rio C, Wolf N, Carleton SA, Gannes LZ (2009) Isotopic ecology ten years after a call for more laboratory experiments. *Biol Rev* 84:91–111
- Myers RJ, Hamilton JB (1951) Regeneration and rate of growth of hairs in man. *Ann NY Acad Sci* 53:562–568
- O'Brien DM, Wooller MJ (2007) Tracking human travel using stable oxygen and hydrogen isotope analyses of hair and urine. *Rapid Commun Mass Spectrom* 21(15):2422–2430
- Passey BH, Cerling TE, Schuster GT, Robinson TF, Roeder BL, Krueger SK (2005) Inverse methods for estimating primary input signals from time-averaged intra-tooth isotope profiles. *Geochim Cosmochim Acta* 69:4101–4116
- Petzke KJ, Fuller BT, Metges CC (2010) Advances in natural stable isotope ratio analysis of human hair to determine nutritional and metabolic status. *Curr Opin Clin Nutr Metab Care* 13(5):532–540
- Rowicka M, Kudlicki A, Tu BP, Otwowski Z (2007) High-resolution timing of cell cycle-regulated gene expression. *Proc Natl Acad Sci (USA)* 104:16892–16897
- Sachs H (1995) Theoretical limits of the evaluation of drug concentrations in hair due to irregular hair growth. *Forensic Sci Int* 70:53–61
- Sachs H (1997) History of hair analysis. *Forensic Sci Int* 84:7–16
- Schwertl M, Auerswald K, Schnyder H (2003) Reconstruction of the isotopic history of animal diets by hair segmental analysis. *Rapid Commun Mass Spectrom* 17:1312–1318
- Selavka CM, Rieders F (1995) The determination of cocaine in hair: a review. *Forensic Sci Int* 70:155–164
- Siegel-Gaskins D, Ash JN, Crosson S (2009) Model-based deconvolution of cell cycle time-series data reveals gene expression details at high resolution. *PLoS Comput Biol* 5(8):e1000460
- Sponheimer M, Robinson T, Ayliffe L, Roeder B, Hammer J, Passey B, West A, Cerling T, Dearing D, Ehleringer J (2003) Nitrogen isotopes in mammalian herbivores: hair $\delta^{15}\text{N}$ values from a controlled feeding study. *Int J Osteoarchaeol* 13:80–87
- Staub C (1995) Analytical procedures for determination of opiates in hair: a review. *Forensic Sci Int* 70:111–123
- Van Scott EJ, Reinertson RP, Steinmuller RJ (1957) The growing hair root of the human scalp and morphological changes therein following ametropin therapy. *J Invest Dermatol* 29:197–204
- Vogel CR (2002) Computational methods for inverse problems. Society for Industrial and Applied Mathematics, University City Science Center, Philadelphia. ISBN-10: 0898715075
- Wainhaus SB, Tzanani N, Dagan S, Miller ML, Amirav A (1998) Fast analysis of drugs in a single hair. *J Am Soc Mass Spectrom* 9:1311–1320
- West AG, Ayliffe LK, Cerling TE, Robinson TF, Karren B, Dearing MD, Ehleringer JR (2004) Short term diet changes revealed using stable carbon isotopes in horse tail-hair. *Funct Ecol* 18:616–624
- Williams LJ, White CD, Longstaffe FJ (2011) Improving stable isotope interpretations made from human hair through reduction of growth cycle error. *Am J Phys Anthropol* 145:125–136
- Wittemyer G, Cerling TE, Douglas-Hamilton I (2009) Establishing chronologies from isotopic profiles in serially collected animal tissues: an example using tail hairs from African elephants. *Chem Geol* 263:3–11
- Wolf N, Carleton SA, Martínez del Rio C (2009) Ten years of experimental animal isotopic ecology. *Funct Ecol* 23(1):17–26